J Geod (2011) 85:931–939
DOI 10.1007/s00190-011-0452-4

ORIGINAL ARTICLE

Ground- and space-based GPS data ingestion into the NeQuick model

C. Brunini · F. Azpilicueta · M. Gende · E. Camilion · A. Aragón-Ángel · M. Hernandez-Pajares · M. Juan · J. Sanz · Dagoberto Salazar

Received: 6 July 2010 / Accepted: 11 February 2011

Abstract This paper presents a technique for ingesting ground- and space-based dual-frequency GPS observations into a semi-empirical global electron density model. The NeQuick-2 model is used as the basis for describing the global electron density distribution. This model is mainly driven by the F2 ionosphere layer parameters (i.e. the electron density, N_mF2, and the height, h_mF2 of the F2 peak), which, in the absence of directly measured values, are computed from the ITU-R database (ITU-R 1997). This database was established using observations collected from 1954 to 1958 by a network of around 150 ionospheric sounders with uneven global coverage. It allows computing monthly median values of N_mF2 and h_mF2 (intra-month variations are averaged), for low and high solar activity. For intermediate solar activity a linear interpolation must be performed. Ground-based GNSS observations from a global network of ∼350 receivers are pre-processed in order to retrieve slant total electron content (sTEC) information, and space-based GPS observations (radio occultation data from the FORMOSAT-3/COSMIC constellation) are pre-processed to retrieve electron density (ED) information. Both, sTEC and ED are ingested into the NeQuick-2 model in order to adapt N_mF2 and h_mF2, and reduce simultaneously both, the observed minus computed sTEC and ED differences. The first experimental results presented in this paper suggest that the data ingestion technique is self consistent and able to reduce the observed minus computed sTEC and ED differences to ∼25–30% of the values computed from the ITU-R database. Although sTEC and ED are both derived from GPS observations, independent algorithm and models are used to compute their values from ground-based GPS observations and space-based FORMOSAT-3/COSMIC radio occultations. This fact encourages us to pursue this research with the aim to improve the results presented here and assess their accuracy in a reliable way.

Keywords Ionosphere · GPS · FORMOSAT-3/COSMIC · NeQuick-2 · ITU-R-database · Data ingestion

C. Brunini (✉) · F. Azpilicueta · M. Gende · E. Camilion
Geodesia Espacial y Aeronomía, Facultad de Ciencias Astronómicas y Geofísicas, Universidad Nacional de La Plata, Paseo del Bosque, s/n, La Plata, Argentina
e-mail: claudiobrunini@yahoo.com

A. Aragón-Ángel · M. Hernandez-Pajares · M. Juan · J. Sanz · D. Salazar
Research group of Astronomy and Geomatics, Applied Mathematics IV Department, Universitat Politecnica de Catalunya, Campus Nord 1-3, Barcelona, Spain

1 Introduction

Researches exploring the potentialities of GPS observations to study the Earth's ionosphere can be traced back to the eighties (e.g. Kleusberg 1986; Feess and Stephens 1987; Lanyi and Roth 1988; Wild et al. 1989). A milestone in that field of research was the establishment of the International GNSS Service (IGS) Ionospheric Working Group (IGS-IWG), in May 1998, which has been producing uninterrupted time series of Global Ionospheric Maps (GIMs) (Feltens and Schaer 1998; Schaer et al. 1996; Manucci et al. 1998; Feltens 1998; Hernández-Pajares et al. 1999). Based on dual-frequency observations from the IGS network, the GIMs provide a world-wide map of the vertical total electron content (vTEC) with a time resolution of 2 h. As a new product, IGS GIMs were cautiously considered by the Aeronomy community but, at present, they are well valued and routinely used for both, scientific and technological studies of the Earth's ionosphere (Hernández-Pajares et al., 2009).

Most TEC models developed within the geodetic community can be characterized as "data-driven models", meaning

that they rely mostly on the information provided by the GNSS data rather than on the chemical and physical processes that actually drive the vTEC distribution. A common way to avoid the formulation of those complex models is to adopt the so-called "thin shell approximation", in which the whole ionosphere is approximated by one (in some cases two) shell(s) of infinitesimal thickness(es) with equivalent vTEC, and a geometrical mapping function is used to relate the satellite-to-receiver slant total electron content (sTEC) to the vTEC on the shell(s) (Manucci et al. 1999). Spatial and temporal variations of vTEC on the shell are reproduced using different kinds of mathematical techniques, e.g. spherical harmonic expansion (Azpilicueta et al. 2005), kriging (Orús et al. 2005), B-spline expansion (Schmidt et al. 2008), etc. The numerical coefficients involved in the mathematical description of the vTEC are estimated from the GNSS observations using some optimization technique (e.g. least squares or Kalman filter when real-time results are desired). Simultaneously to the mathematical coefficients, the so-called inter frequency biases (IFBs) must be estimated in order to account for frequency-dependent delays that are not produced by the ionosphere but by the GNSS satellites and receivers hardware and firmware (Sardon et al. 1994). An alternative to the thin shell approach is the "ionospheric tomography" (Hernández-Pajares et al. 1999). In this case the ionosphere is parcelled in 3-dimensional cells or "voxels", and the electron density (ED) inside each voxel is estimated from the satellite-to-receiver ray paths that pass through it. Mathematical constraints must be imposed to fill up voxels that are not crossed by any ray path.

Another milestone for the ionospheric research based on GPS observations was the GPS/MET experiment, conducted by the University Corporation for Atmospheric Research (UCAR), which placed a dual-frequency GPS receiver on board a low-Earth orbiter (LEO) satellite (Hajj et al. 1994). This and other dual-frequency GPS receivers flying on LEO satellites (e.g. SAC-C, CHAMP, GRACE, FORMOSAT-3/COSMIC, etc.) put the so-called "radio occultation techniques" into practice and made possible the use of GPS observations to derive information about the ED distribution at different heights in the ionosphere (Jakowski et al. 2004). These techniques are also based on "data-driven model" which can be classified into two main groups: the already mentioned "ionospheric tomography" (Leitinger et al. 1997) and the "Abel transform" (Schreiner et al. 1999). The last one retrieves the ED from either the bending angle or the sTEC of the LEO-GPS ray path. The classical formulation of the Abel transform technique relies upon the assumption of spherical symmetry of the ED distribution, but an improved version of it overcame that assumption by including information about the horizontal gradients present in the neighboring area of the radio occultation event. Such a kind of information can be extracted, for instance, from the vTEC distribution provided by the IGS GIMs (Hernández-Pajares et al. 2000).

In spite of its relative simplicity, GNSS-data driven models are able to produce a reliable representation of both, ED and TEC, even with better accuracy than other models founded in more sophisticated empirical or chemical and physical basements. Even if true, this fact does not implies at all that the efforts for improving the last kind of models lack of sense: far from this, the aeronomy community is convinced that only a full synergy between models and data can help to understand the great complexity of ionospheric processes and predict the main ionospheric variables. The techniques being developed to exploit that synergy can be classified into two major groups: "data assimilation" and "data ingestion". The first one is based on the use of the so-called "first principle ionospheric models", which have to solve a non linear and coupled system of differential equations for each one of the most abundant ion species in the Earth's atmosphere (Schunk 2002; Wang et al. 2004). That system accounts for the mass conservation principle through the continuity equation, the momentum conservation principle through the Navier-Stokes equation, the energy conservation principle through the temperature equation, etc. Solving the system requires the use of models for computing the main driving forces, such as the neutral winds, the gravity and Lorenz forces, etc. The integration of the differential equation system originates a number of initial and boundary conditions that are estimated by means of the data assimilation process, which is usually done, state by state of the model, by means of a Kalman filter. Data ingestion differs from data assimilation by the fact that physical and chemical models are simplified and parameterized in terms of a given set of model parameters, which are estimated in order to minimize the deviations between observed and computed values. Simplified models can be based either on empirical facts (e.g. IRI (Bilitza 2001), NeQuick (Radicella and Leitinger 2001), etc.) or physical laws (SUPIM (Bailey et al. 1997), SAMI2 (Huba et al. 2000), etc.).

In this contribution, we present a technique to ingest GPS-derived sTEC and FORMOSAT-3/COSMIC-derived ED into the NeQuick empirical model. In Sect. 2 we describe how the NeQuick model is parametrized in order to fulfil the requirements of the data ingestion technique; in Sect. 3 we describe the data ingestion technique itself; in Sect. 4 we present the obtained results which constitute the first assessment regarding the goodness of the data ingestion technique; finally, we summarize the main conclusions learned from this research, including some interesting possibilities to further improve the data ingestion technique here presented that will be investigated in forthcoming works.

2 Base model for data ingestion

Version 2 of the NeQuick model (Nava et al. 2008) is used as the basis to describe the time varying global ED distribution at global scale. This version is a recent evolution of the one that is being implemented by the Galileo GNSS for correcting the ionospheric range delay error for single-frequency operation. NeQuick-2 describes the vertical profile of ED by means of the superposition of six semi-Epstein functions that represent the lower and upper parts of the E and F1 layers, the lower part of the F2 layer, and the topside ionospheric profile. The functions are anchored to the ED, N_m, and the height, h_m, of the corresponding layer peak, which can be either measured (with ionospheric sounders) or modelled. Besides, the thickness of each layer is modelled with different functions for its lower and upper parts.

Despite the existence of three anchor points in the NeQuick-2 formulation, the shape of the profile is dominated by the F2 parameters, N_mF2 and h_mF2. In the absence of measurements NeQuick-2 proceeds in the same way as the IRI model and computes values for those parameters based on a climatological database. As it will be soon explained, this database allows computing monthly mean values of the critical frequency, f_0F2, and the transfer parameter, $M_{3000}F2$ and, from them, NeQuick-2 computes N_mF2 using the simple relation:

$$N_mF2 = \frac{f_0F2^2}{80.6}, \tag{1}$$

and h_mF2 using the Dudeney (1974) formulae in connection with $M_{3000}F2$ and the f_0F2/f_0E ratio:

$$h_mF2 = \frac{1{,}490 \cdot M_{3000}F2 \cdot \sqrt{\frac{0.0196 \cdot M_{3000}F2^2+1}{1.2967 \cdot M_{3000}F2^2-1}}}{M_{3000}F2 + \Delta M} - 1.76, \tag{2.a}$$

where the ΔM factor is given by

$$\Delta M = \begin{cases} \dfrac{0.253}{\frac{f_0F2}{f_0E} \cdot \frac{e^{20\cdot\left(\frac{f_0F2}{f_0E}-1.75\right)}+1.75}{e^{20\cdot\left(\frac{f_0F2}{f_0E}-1.75\right)}+1}-1.215} - 0.012, & \text{if the E layer is present} \\ -0.012, & \text{if the E layer is not present} \end{cases} \tag{2.b}$$

The critical frequency and the transfer parameter in the Eqs. (2) are given in MHz, the ED in electrons/m^3 and the height in km.

According to the mapping technique developed by Jones and Gallet (1965), the diurnal variation of f_0F2 and $M_{3000}F2$ is given by Fourier series:

$$\Omega = a_0 + \sum_{j=1}^{J} a_j \cdot cos\,(j \cdot t) + b_j \cdot \sin\,(j \cdot t) \tag{3.a}$$

where Ω is the parameter to be mapped; t is UT; and J is the maximum number of harmonics for mapping the diurnal variation ($J = 6$ for f_0F2 and $J = 4$ for $M_{3000}F2$). The geographic variation of these parameters is accounted for the Fourier coefficients in the form

$$a_j = \sum_{k=0}^{K} U_{2j,k} \cdot G_k,\ j \geq 0;\ b_j = \sum_{k=0}^{K} U_{2j-1,k} \cdot G_k,\ j \geq 1, \tag{3.b}$$

where $K = 75$ for f_0F2 and $K = 49$ for $M_{3000}F2$; U are the numerical coefficients of the expansion [998 U_f coefficients for f_0F2 (13 from Eq. 3.a by 76 from Eq. 3.b) and 450 U_M coefficients for $M_{3000}F2$(9 from Eq. 3.a by 50 from Eq. 3.b)]; and G are special functions whose explicit form depends on the k index, for example

$$G_{54} = \sin^8(\mu) \cdot \cos^2(\varphi) \cdot \cos(2 \cdot \lambda), \tag{3.c}$$

where φ and λ are the geographic latitude and longitude and μ is the so-called "modip" latitude defined as

$$\mu = atan\left(\frac{I}{\sqrt{\cos\varphi}}\right), \tag{3.d}$$

I is the magnetic dip at 350 km above the Earth's surface.

The maximum number of terms for mapping the diurnal and geographic variations of f_0F2 and $M_{3000}F2$ (J and K in Eqs. 3.a, 3.b) was established by fitting a set of measured values with an increasing number of terms until the root mean square difference between data and model did not further improve. The final remaining root mean square was about 0.5 MHz for f_0F2 and 0.5 for $M_{3000}F2$ (see Jones and Gallet 1965 for details).

The particular G functions chosen by Jones and Gallet as bases for mapping the geographical variability of f_0F2 and $M_{3000}F2$ seem to be very well adapted for f_0F2. With only 998 coefficients, the technique is able to map very well the sharp peaks and the deep valley between these peaks that f_0F2 exhibits in response to the Appleton anomaly (features that are not so well mapped with other base-function such as the associated Legendre functions). Besides, the use of the modip latitude helps to cope with the distortion that the Earth's magnetic field causes on this complex structure.

3 Data ingestion technique

NeQuick-2 relies upon the climatological database provided by the Radio Communication Sector of the International Telecommunication Union, namely the ITU-R database (ITU-R 1997), to compute the U coefficients required by the f_0F2 and $M_{3000}F2$ expansions given in Eq. (3). This database was established using observations collected from 1954 to 1958 by a network of around 150 ionospheric sounders unevenly distributed around the world and provides two sets of U coefficients, one for low and another for high solar

activity, for every month of the year. The solar activity is characterized by the 12-month running mean value of the monthly mean sunspot number, R_{12}. For a given month and R_{12} value, the U coefficients must be linearly interpolated from the tabulated values, which correspond to $R_{12} = 0$ (low) and $R_{12} = 100$ (high solar activity)

The outdated ITU-R database, the monthly median averages that do not account for the day-by-day variations, the linear interpolation used to account for the solar activity, and the intrinsic errors of the database, cause significant differences between the computed and the actual values of f_0F2 and $M_{3000}F2$, thus inducing large errors on NeQuick-2 (e.g. Jodogne et al. 2004). Under this premise we look for a data ingestion technique that allows using GPS-sTEC and FORMOSAT-3/COSMIC-ED to compute corrections ΔU_f and ΔU_M to the $U_{f,0}$ and $U_{M,0}$ values computed from the ITU-R database, so that the corrected values,

$$\begin{aligned} U_{f,i} &= U_{f,0,i} + \Delta U_{f,i} \qquad i = 1, 2, \ldots, 988 \\ U_{M,i} &= U_{M,0,i} + \Delta U_{M,i}, \quad i = 1, 2, \ldots, 450 \end{aligned} \tag{4.a}$$

can reduce the differences between observed and computed values. With this idea in mind, the NeQuick-2 model is parametrized in terms of the $998 + 450 = 1,448$ U coefficients:

$$\begin{aligned} N_{eN} &= F\left(f_0F2(U_{f,1}, \ldots, U_{f,988}),\right. \\ &\quad \left. M_{3000}F2(U_{M,1}, \ldots, U_{M,450})\right) \\ &\cong F\left(f_0F2(U_{f,0,1}, \ldots, U_{f,0.988}),\right. \\ &\quad \left. M_{3000}F2(U_{M,0.1}, \ldots, U_{M,0.450})\right) \\ &\quad + \sum_{i=1}^{988} \frac{\partial N_{eN}}{\partial f_0F_2} \cdot \frac{\partial f_0F_2}{\partial U_{f,i}} \cdot \Delta U_{f,i} \\ &\quad + \sum_{i=1}^{450} \frac{\partial N_{eN}}{\partial M_{3000}F2} \cdot \frac{\partial M_{3000}F2}{\partial U_{M,i}} \cdot \Delta U_{M,i}, \end{aligned} \tag{4.b}$$

where the $\frac{\partial N_{eN}}{\partial f_0F_2}$ and $\frac{\partial N_{eN}}{\partial M_{3000}F_2}$ derivatives are numerically computed and the other derivatives are analytically computed from Eq. (3):

$$\begin{aligned} &\frac{\partial f_0F_2}{\partial U_{f,2j,k}} = G_k \cdot \cos(j \cdot t); \quad \frac{\partial M_{3000}F2}{\partial U_{M,2,j,k}} = G_k \cdot \cos(j \cdot t) \\ &\frac{\partial f_0F_2}{\partial U_{f,2j-1,k}} = G_k \cdot \sin(j \cdot t); \frac{\partial M_{3000}F2}{\partial U_{M,2,j-1,k}} = G_k \cdot \sin(j \cdot t). \\ &\mathrm{k} = 1, \ldots, 75 \quad \text{and} \quad \mathrm{k} = 1, \ldots, 49 \quad \text{and} \\ &\mathrm{j} = 1, \ldots, 6; \quad \mathrm{j} = 1, \ldots, 4 \end{aligned} \tag{4.c}$$

The data ingestion is performed by means of an adaptative and robust Kalman filter through which the set of $998 + 450 = 1,448U$ coefficients is updated every hour. Two kinds of observations were simultaneously ingested by the filter into the NeQuick-2 model:

- GPS derived sTEC, which give rise to the following equation of observation:

$$\begin{aligned} sTEC_G &\cong \int_\gamma F\left(f_0F2(U_{f,0,1}, \ldots, U_{f,0,988}),\right. \\ &\quad \left. M_{3000}F2(U_{M,0,1}, \ldots, U_{M,0,450})\right) \cdot d\gamma \\ &\quad + \sum_{i=1}^{988} \left(\int_\gamma \frac{\partial N_{eN}}{\partial f_0F_2} \cdot \frac{\partial f_0F_2}{\partial U_{f,i}} \cdot d\gamma \right) \cdot \Delta U_{f,i} + \beta_R + \beta_S, \end{aligned} \tag{4.d}$$

  where γ is the satellite-to-receiver line-of-sight, and β_S and β_R are the GPS satellite and receiver inter-frequency biases.
- FORMOSAT-3/COSMIC derived ED, which give rise to the following equation of observation:

$$\begin{aligned} N_{eF} &\cong F\left(f_0F2(U_{f,0,1}, \ldots, U_{f,0,988}),\right. \\ &\quad \left. M_{3000}F2(U_{M,0,1}, \ldots, U_{M,0,450})\right) \\ &\quad + \sum_{i=1}^{988} \frac{\partial N_{eN}}{\partial f_0F_2} \cdot \frac{\partial f_0F_2}{\partial U_{f,i}} \cdot \Delta U_{f,i} \\ &\quad + \sum_{i=1}^{450} \frac{\partial N_{eN}}{\partial M_{3000}F2} \cdot \frac{\partial M_{3000}F2}{\partial U_{M,i}} \cdot \Delta U_{M,i}. \end{aligned} \tag{4.e}$$

  It is worth pointing out that Eq. (4.d) does not contain corrections to the $M_{3000}F2$ parameter. This is because the ground-based GPS sTEC does not provide enough information on the ED variation with height and are hence almost insensitive to $M_{3000}F2$.

4 Goodness assessment of the data ingestion technique

The results presented in this section are based on 10 days of continuous observations, from Jan 6 to 15, 2007, a period characterized by low solar activity ($R_{12} \leq 22$) and quiet geomagnetic conditions ($Dst \geq -26$). As already mentioned, two kinds of observations were simultaneously ingested by the Kalman filter into the NeQuick-2 model: $\sim 5 \times 10^5$ sTEC per hour derived from the observations provided by $\sim$ 350 stations belonging to the IGS network (assuming $15 - 30^s$ sampling rate and $\sim$ 8 simultaneous satellites per epoch) and $\sim 2 \times 10^4$ ED per hour derived from $\sim$ 900 FORMOSAT-3/COSMIC radio ocultations per day.

GPS observations were pre-processed with the La Plata ionospheric model (LPIM) (Azpilicueta et al. 2005) in order to derive unambiguous but uncalibrated sTEC. LPIM computes the geometry-free linear combination from both, carrier- and code-phase dual-frequency GPS observations; detects and corrects (when possible) carrier-phase cycle slip;

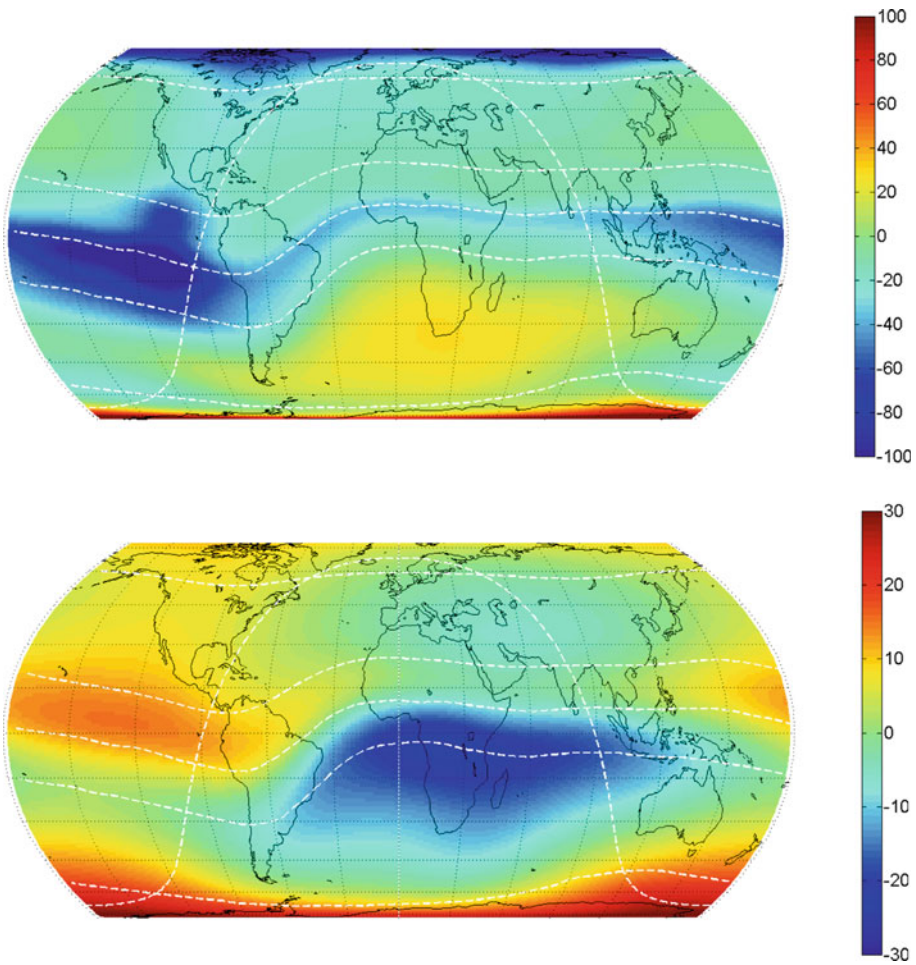

Fig. 1 Percentile value of the corrections to the f_0F2 (*upper panel*) and $M_{3000}F2$ (*bottom panel*) values computed from the ITU-R database

and estimates and reduces carrier-phase ambiguities by levelling the carrier- to the code-phase geometry-free linear combination. These pre-processes produce carrier-phase derived sTEC, free from ambiguities and cycle slips but affected by the GPS satellite and receiver inter-frequency biases, β_S and β_R.

FORMOSAT-3/COSMIC radio occultation data were processed by means of the improved Abel inversion technique to retrieve ED from the dual frequency GPS observations collected by the receiver on board the LEOs (see details in Aragón-Ángel et al. 2009). The technique used in this research overcomes the limitation imposed by the spherical symmetry assumption that underlies on the classical Abel inversion technique, which is equivalent to neglect the horizontal gradients of the actual ED distribution and considering only its variation with height. According to the "separability hypothesis" introduced by Hernández-Pajares et al. (2000), the ED distribution can be expressed as the product of the vTEC distribution, which accounts for the horizontal ED gradients, and the "shape function", which accounts for the ED dependence on height. The IGS GIMs supply the necessary information regarding the vTEC distribution while the shape function, and hence the ED, is estimated from the L_1 carrier-phase excess.

Just to provide an example, Fig. (1) illustrates the geographical variability of the corrections to f_0F2 (upper panel) and $M_{3000}F2$ (bottom panel), at 12^h UT of one of the 10 days computed in this research. More specifically, the figure shows the percentile value of these corrections in terms of the values computed from the ITU-R database, i.e. $100 \times (f_0F2 - f_0F2_0)/f_0F2_0$ and $100 \times (M_{3000}F2 - M_{3000}F2_0)/M_{3000}F2_0$. Dashed white lines represent the modip parallels of $\pm 60°, \pm 30°$ and $0°$ that roughly delimit the high-, mid- and low-latitude ionosphere. The solar terminator (i.e. the imaginary line that divides the day from the night-sector) is also depicted with a dashed white line. We do not attempt here to discuss the physical significance of the corrections computed for a particular day.

Nevertheless, some general remarks may be interesting at this point:

- the f_0F2 correction reaches values around -100% at high North latitude and $+100\%$ at high South latitude; at mid latitude and day-time the correction is around -15% in the Northern and $+20\%$ in the Southern Hemisphere; at low latitude and night-time the correction is around -40%.
- the $M_{3000}F2$ correction is around $+5\%$ at high North latitude and reaches values greater than $+20\%$ at high South latitude; at mid and low latitude and day-time the correction is around -15% in the Southern Hemisphere; at mid and low latitude and night-time the correction is around $+15\%$ in the Northern Hemisphere.

Figure (2) shows typical examples extracted from the $\sim 9,000$ radio occultations analysed in this work. The figures show the ED (electron/m^3) in the x axe and the height (kilometres) in the y axes. The three panels on the left-hand-side correspond to night-time radio occultations and the three panels in the right-hand-side correspond to day-time radio occultations. From top to bottom the panels correspond to high-, mid- and low-latitude radio occultations. The points represent the FORMOSAT-3/COSMIC derived ED, the dashed line represents the ED from NeQuick before data ingestion, and the solid line represents the ED from NeQuick after data ingestion. In all the cases presented in this figure, the data ingestion technique is able to significantly reduce the deviations between the observed and computed ED. This fact is confirmed by the statistics presented in Fig. (3), which show the distribution of the observed minus computed ED deviations (in electron/m^3 in the x axis) and percentage of samples (in the y axis) for the $\sim$9000 radio occultations analysed in this work. The goodness of the technique is evident when the distributions after (solid line) and before (dashed line) data ingestion are compared: both, the mean value and the standard deviation are reduced from $-2.9\times10^{10}\pm7.0\times10^{10}$ to $0.1\times10^{10}\pm2.1\times10^{10}$electron/m^3.

Figure (4) shows typical examples extracted from the $\sim$ 350 ground-based GPS stations considered in this study. Each group of three panels of this figure shows sTEC variations (in the y axis, in TECu) as function of the local time (x axis, in hour) for selected stations located, from top to bottom, in high-, mid- and low-latitude regions, for one of the 10 days analysed in this work. The upper panel of each group shows the sTEC computed from NeQuick-2 after data ingestion, while the middle and bottom panels show the observed minus computed deviations before and after data ingestion. In all the cases presented in this figure, the data ingestion technique is able to significantly reduce the deviations between the observed and computed sTEC. This fact is confirmed by the statistics presented in Fig. (5), which shows

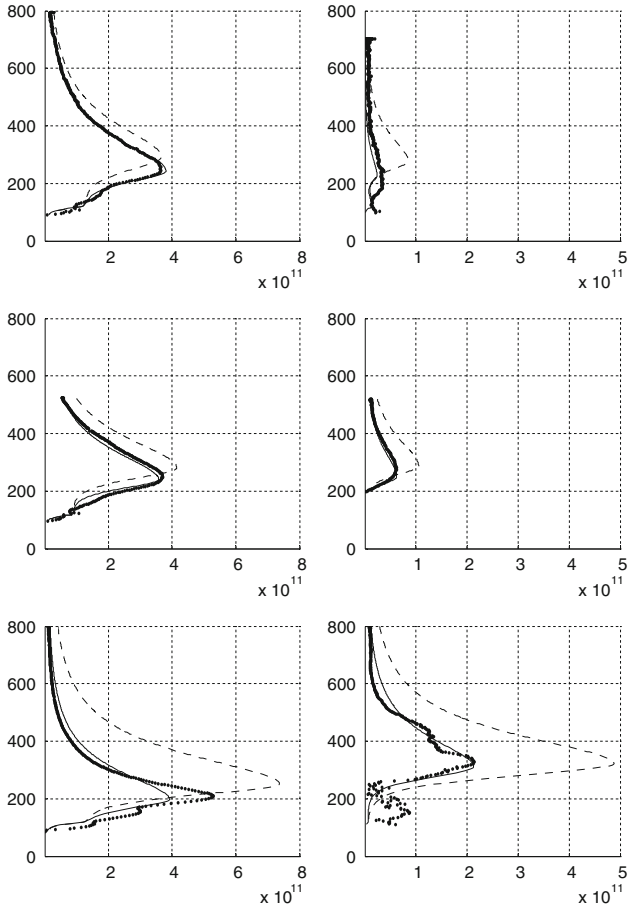

Fig. 2 ED profiles for selected radio occultations for day-time (*right*) and night-time (*left*); for high, mid and low latitude (from *top to bottom*); from FORMOSAT-3/COSMIC data (*points*) and from NeQuick before (*dashed line*) and after (*solid line*) data ingestion

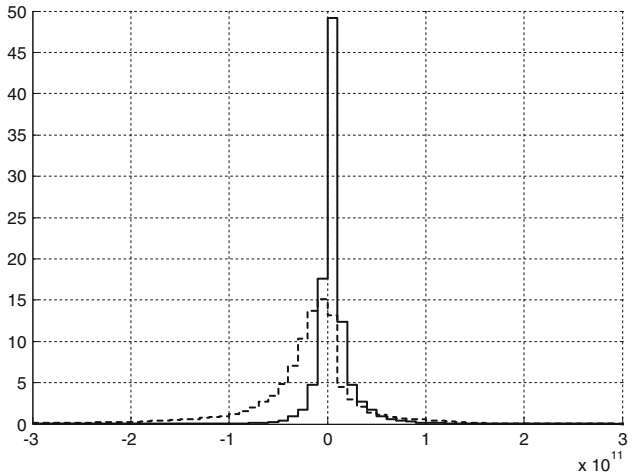

Fig. 3 Percentile distribution of the observed minus computed ED deviations before (*dashed line*) and after (*solid lines*) data ingestion

the distribution of the observed minus computed sTEC deviations (in TECu, in the x axis) and the percentage of samples

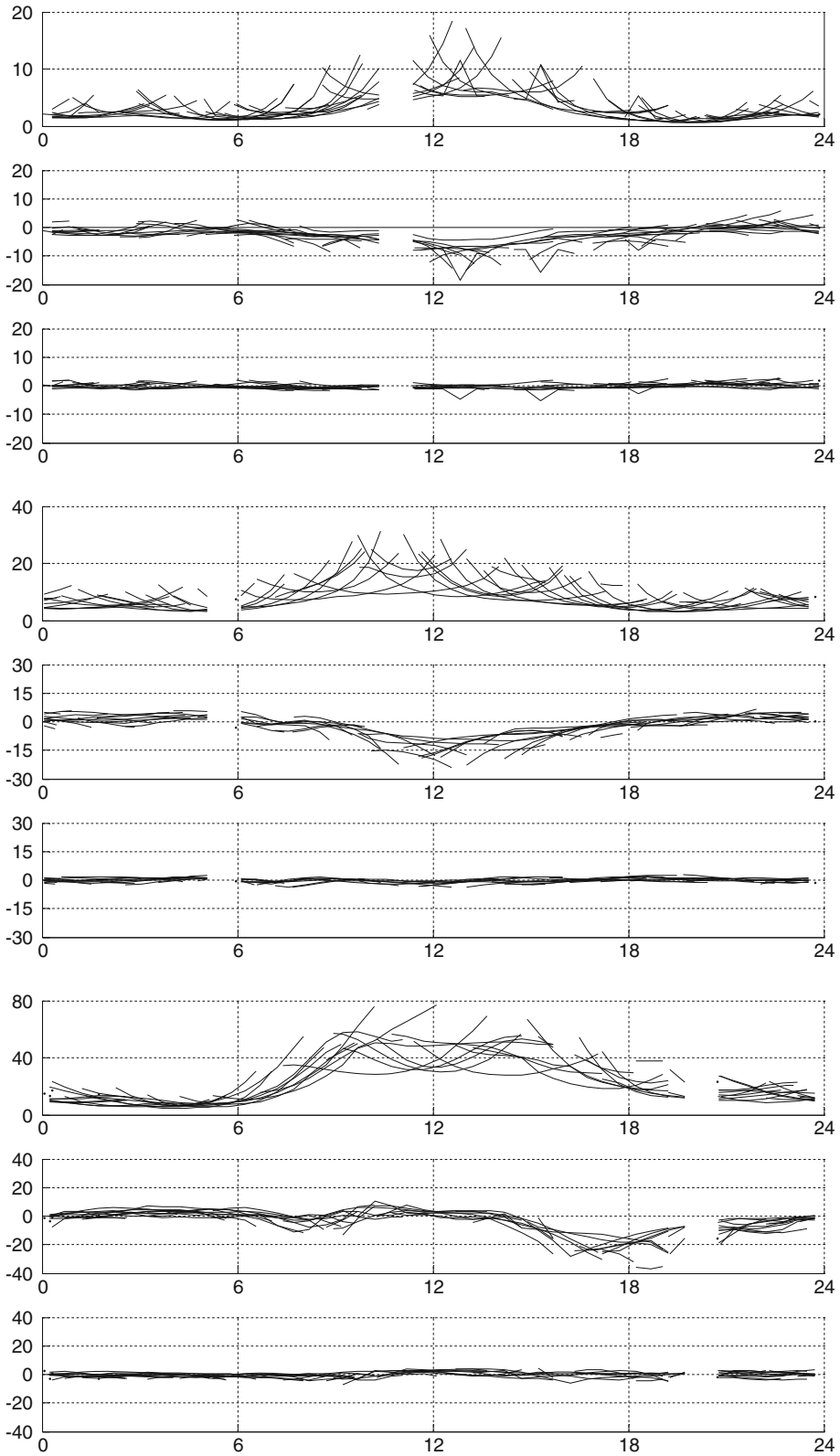

Fig. 4 Daily sTEC variation for selected stations at high, mid and low latitude (from *top to bottom*); the *upper panel* of each group shows the sTEC from NeQuick-2 after data ingestion, while the middle and *bottom panels* show the observed minus computed deviations before and after data ingestion (data gaps in the plots are due to limitations of the processing software to handle the transition between 24 to 0 UT)

(in the y axis) for the ~ 350 ground-based GPS stations and 10 days of observations analysed in this work. The goodness of the technique is evident when the distributions after (solid line) and before (dashed line) data ingestion are compared: both, the mean value and the standard deviation are reduced from -1.5 ± 5.1 to -0.1 ± 1.5 TECu.

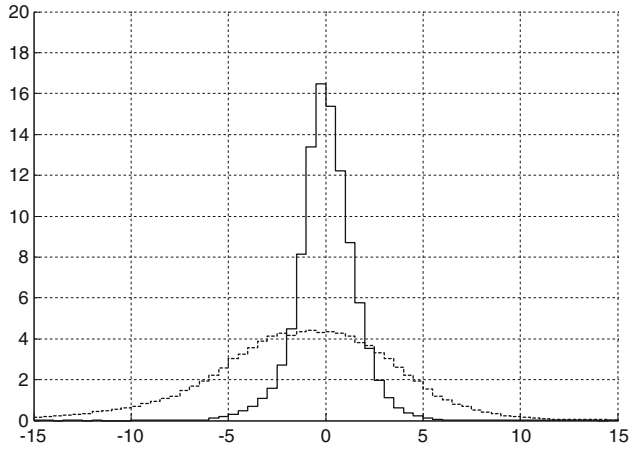

Fig. 5 Percentile distribution of the observed minus computed sTEC deviations before (*dashed line*) and after (*solid lines*) data ingestion

5 Conclusions and further works

This paper presented a global-scale technique to ingest ground-based GPS-derived sTEC and space-based FORMOSAT-3/COSMIC derived ED into the NeQuick-2 model. The technique relies upon the estimation of corrections to the ITU-R climatological database coefficients in order to simultaneously minimize the observed minus computed sTEC and ED differences. The first experimental results presented in this paper suggested that the technique is self consistent and able to reduce the observed minus computed differences to $\sim 25 - 30\%$ of the values computed from the ITU-R database for both, ground- and space-based data. It is worth mentioning that ground-based sTEC and space-based ED were derived from different algorithms and models.

In the future we intend to analyse the performance of the technique under different solar and geomagnetic conditions; validate the obtained sTEC and ED by comparing them to different data sources (e.g. TOPEX, Jason, ionospheric sounders, etc.); and validate the f_0F2 and $M_{3000}F2$ parameters computed with this technique by comparing them to ionospheric sounders and incoherent scatter radar determinations. Besides, we intend to change the parameterization of the NeQuick-2 model using h_mF2 instead of $M_{3000}F2$. As it was already mentioned in the second section of this paper, the base functions used by the Jones and Gallet's technique is well suited for mapping the sharp peaks and deep valley of f_0F2 in the region of the Appleton anomaly, but $M_{3000}F2$ exhibits a different behaviour that could be better mapped using different base functions (e.g. Legendre's associated functions). In addition, the derivation of h_mF2 from $M_{3000}F2$ using the Dudeney's formulae (Eqs. 2) makes the estimation the $M_{3000}F2$ corrections rather unstable.

References

Aragón-Ángel A, Hernández-Pajares M, Juan JM, Sanz J (2009) Improving the Abel transform inversion using bending angles from FORMOSAT-3/COSMIC, GPS Solut, doi:10.1007/s10291-009-0147-y

Azpilicueta F, Brunini C, Radicella SM (2005) Global ionospheric maps from GPS observations using modip latitude. JASR, Elsevier, Amsterdam (36):552–561

Bailey GJ, Balan N, Su YZ (1997) The Sheffield University plasmasphere ionosphere model: a review. J Atmos Sol Terr Phys 59:1541–1552

Bilitza D (2001) International Reference Ionosphere 2000. Radio Sci 36(2):261–275

Dudeney JR (1974) A Simple Empirical Method for Estimating the Height of the F2-Layer at the Argentine Islands Graham Land, Science Report No 88, British Antarctic Survey, London, UK

Feess WA, Stephens SG (1987) Evaluation of GPS ionospheric time delay model. IEEE Trans Aerosp Electron Syst 23(3):332–338

Feltens J (1998) Chapman profile approach for 3-D global TEC representation. In: Dow JM, Kouba J, Springer T (eds) Proceedings of the IGS Analysis Center Workshop, Darmstadt pp 285-297

Feltens J, Schaer S (1998) IGS products for the ionosphere. In: Dow JM, Kouba J, Springer T (eds) Proceedings of the IGS Analysis Center Workshop, 225-232, Darmstadt, 1998

Hajj GA, Ibanez-Meier R, Kursinski ER, Romans LJ (1994) Imaging the ionosphere with global positioning system. Int J Imaging System Technology 5:174–184

Hernández-Pajares M, Juan JM, Sanz J (1999) New approaches in global ionospheric determination using ground GPS data. J Atmos Sol Terr Phys 61:1237–1247

Hernández-Pajares M, Juan JM, Sanz J (2000) Improving the Abel inversion by adding ground GPS data to LEO radio occultations in ionospheric sounding. Geop Res Lett 27(16) 2473–2476

Hernández-Pajarez M, Juan JM, Sanz J, Orus R, Garcia-Rigo A, Feltens J, Komjathy A, Schaer SC, Krankowski A (2009) The IGS VTEC map: a reliable source of ionospheric information since 1998. J Geod 83:263–275

Huba JD, Joyce G, Fedder JA (2000) Sami2 is another model of the ionosphere (SAMI2): a new low-latitude ionosphere model. J Geophys Res 105(A10), 23, 035-23,054

ITU-R (1997) Recommendation ITU-R P.1239, ITU-R reference ionospheric characteristics, International Telecommunications Union, Radio - Communication Sector, Geneva

Jakowski N, Leitinger R, Angling M (2004) Radio occultation techniques for probing the ionosphere, Ann Geophys, Suppl. 47(2/3):1049-1066

Jodogne JC, Nebdi H, Warnant R (2004) GPS TEC and ITEC from digisonde data compared with NEQUICK model. Adv Sapce Res 2:269–273

Jones WB, Gallet RM (1965) The representation of diurnal and geographical of ionospheric delay by numerical methods. Telecomm J 32:18

Kleusberg A (1986) Ionospheric propagation effects in geodetic relative GPS positioning. Manuscripta Geodaetica 11:256–261

Lanyi GE, Roth T (1988) A comparison of mapped and measured total ionospheric electron content using Global Positioning System and beacon satellite observations. Radio Sci 23(4):483–492

Leitinger R, Ladreiter HP, Kirchengast G (1997) Ionosphere tomography with data from satellite reception of GNSS signals and ground reception of NNSS signals. Radio Sci 32(4):1657–1669

Manucci AJ, Iijima BA, Lindqwister UJ, Pi X, Sparks L, Wilson BD (1999) GPS and ionosphere, revised submission to URSI reviews of Radio Sci, Jet Propulsion Laboratory, Pasadena, California

Manucci AJ, Wilson BD, Yuan DN, Ho CM, Lindqwister UJ, Runge TF (1998) A global mapping technique for GPS-derived ionospheric total electron-content measurements. Radio Sci 33(3):565–582

Nava B, Coïsson P, Radicella SM (2008) A New version of the NeQuick ionosphere electron density model. J Atmos Sol Terr Phys, pp. 1856–1862 doi:10.1016/j.jastp.2008.01.015

Orús R, Hernández-Pajares M, Juan JM, Sanz J (2005) Improvement of global ionospheric VTEC maps by using kriging interpolation technique. J Atmos Sol Terr Phys 67(16):1598–1609

Radicella SM, Leitinger R (2001) The evolution of the DGR approach to model electron density profiles. Adv Space Res 27(1):35-40

Sardon E, Rius A, Zarraoa N (1994) Estimation of the transmitter and receiver differential biases and the ionospheric total electron content from Global Positioning System observations. Radio Sci 29:577–586

Schaer S, Beutler G, Rothacher M, Soringer T (1996) Daily global ionosphere maps based on GPS carrier phase data routinely produced by the CODE Analysis Center. In: Proceedings of the IGS Analysis Center Workshop, Silver Spring

Schmidt M, Bilitza D, Shum CK, Zeilhofer C (2008) Regional 4-D modeling of the ionospheric electron density. Adv Space Res 42:782–790

Schreiner WS, Sokolovskiy SV, Rocken C, Hunt DC (1999) Analysis and validation of GPSMET radio occultation data in the ionosphere. Radio Sci 34:949–966

Schunk RW (2002) Global Assimilation of Ionospheric Measurements (GAIM), paper presented at Ionospheric Effects Symposium, Office of Naval Research, Alexandria, VA

Wang C, Hajj G, Pi X, Rosen IG, Wilson B (2004) Development of the global assimilative ionospheric model, Radio Sci, 39, doi:10.1029/2002RS002854

Wild U, Beutler G, Gurtner W, Rothacher M (1989) Estimating the ionosphere using one or more dual frequency GPS receivers. In: Proceedings of the Fifth International Geodetic Symposium on Satellite Positioning, Las Cruces, pp 724-736